# High-Power Narrow Linewidth Distributed Feedback Lasers With an Aluminium-Free Active Region Emitting at 852 nm

F.-J. Vermersch, V. Ligeret, S. Bansropun, M. Lecomte, O. Parillaud, M. Calligaro, M. Krakowski, and G. Giuliani

***Abstract*—In this letter, we demonstrate the design, fabrication, and characterization of single-mode distributed feedback (DFB) lasers emitting at 852 nm for atomic clocks and spatial applications. The epitaxial structure comprises an aluminium-free active region with the DFB fabrication technology based on an epitaxial regrowth concept. Initial results carried out on uncoated broad-area devices showed low internal losses ($<3$ cm$^{-1}$), a high internal efficiency (95%), and for antireflection/high-reflectivity coated broad-area lasers, an output optical power of 5.5 W was measured at 8.5 A. Ridge waveguide structures were then fabricated with a ridge width of 4 $\mu$m showing typical single spatial mode emission with the $M^2$ factor $<1.5$. Based on these preliminary results, DFB ridge waveguides were then processed and characterized. Single-mode emission was achieved at 852.12 nm corresponding to the $D_2$ cesium transition, with an optical output power of 40 mW at 140 mA. Linewidth measurement was also carried out on these devices with a linewidth of 0.9 MHz measured at 70 mA.**

***Index Terms*—Atomic clocks, cesium pumping, distributed feedback (DFB) lasers, laser noise, semiconductor laser diode.**

## I. Introduction

SINCE THE introduction of atom optical pumping or laser-cooling techniques, the enhancement of high-power lasers with excellent spectral and spatial quality has been an important research subject. Laser sources emitting at 852 nm, corresponding to the $D_2$ cesium transition, are of particular interest for applications in interferometry and atomic clocks. For atomic clocks on a conventional bench, a common Fabry–Pérot diode laser is placed together with a grating into an external cavity configuration. This setup provides the essential low linewidth, but with limited output power. A master–slave configuration with an amplifying high-power broad-area laser diode is hence necessary to obtain the required power. This technique presents difficulties for spatial applications because of the expensive needs for thermal stabilization, precise and critical optical alignment, and mechanical stability. An alternative approach with a less complex optical setup is to realize a monolithically integrated system based on a distributed feedback (DFB) laser which is monomode spatially and longitudinally. However, in order to use the DFB approach as a viable alternative for spatial or air-borne applications, high output power in a single spatial and longitudinal mode with a spectral linewidth of less than 1 MHz need to be achieved.

Single-mode performance in the 850-nm wavelength range has been achieved using DFB lasers fabricated in the AlGaAs–GaAs material system [1], [2]. However, the use of an InGaAsP active region offers an attractive alternative to this conventional AlGaAs-based design with a much better reliability [3]–[6]. This factor is important for high-power and spatial applications. Another advantage of the aluminium-free system is the easier implementation of epitaxial regrowth compared to an AlGaAs-based system. This is a particularly important issue for the fabrication of a single frequency and single spatial mode operation with a DFB laser structure, based on the epitaxial regrowth concept.

## II. Device Fabrication

The laser structures have been grown on an n-type-doped (100) GaAs substrate by metal–organic vapor phase epitaxy (MOVPE) at reduced pressure in a multiwafer Aixtron reactor. The source materials are arsine and phosphine as V element precursors and trimethylaluminum, trimethylgallium, and trimethylindium as III element precursors. In order to calibrate the amount of strain for the InGaAsP quantum well, its thickness, and the photoluminescence (PL) wavelength, a test structure containing three quantum wells is grown under the same conditions as for the final laser structure. Special attention has been paid to the material quality of the quantum wells, assessed by the full-width at half-maximum (FWHM) and intensity of the PL peaks. High-resolution X-ray diffraction measurements were performed and compared with simulated rocking curves, indicating the strain in the quantum well is around 0.6%.

The device uses a separate confinement heterostructure. The DFB laser presented here was grown in two steps. The first step consisted of a n-GaAs buffer, n-AlGaInP ($\mathrm{Al}_{25\%}$) cladding, a 450-nm n-GaInP ($\mathrm{Ga}_{51\%}$) waveguide, an 8-nm-thick compressively active strained InGaAsP quantum well embedded in $Q1.6$ barrier layers, 450-nm p-GaInP waveguide, p-AlGaInP cladding and gratings layers. The waveguide is a large optical cavity of 1 $\mu$m. The confining layers consist of p- and n-doped AlGaInP

Manuscript received February 8, 2008; revised April 3, 2008. This work was supported by the French Center for Spatial Studies: CNES.

F.-J. Vermersch is with Saint Gobain Research, 93303 Aubervilliers, France.

V. Ligeret, M. Lecomte, O. Parillaud, M. Calligaro, and M. Krakowski are with Alcatel Thales 3-5lab, 91767 Palaiseau, France (e-mail: vincent.ligeret@3-5lab.fr).

S. Bansropun is with Thales Research and Technology, 91767 Palaiseau, France.

G. Giuliani is with the Dipartimento di EleTronica, Universita di Pavia, 27100 Pavia, Italy.

Color versions of one or more of the figures in this letter are available online at http://ieeexplore.ieee.org.

Digital Object Identifier 10.1109/LPT.2008.924903

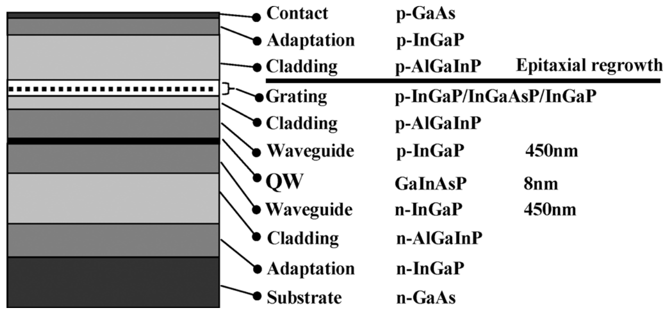


Fig. 1. Vertical laser structure.

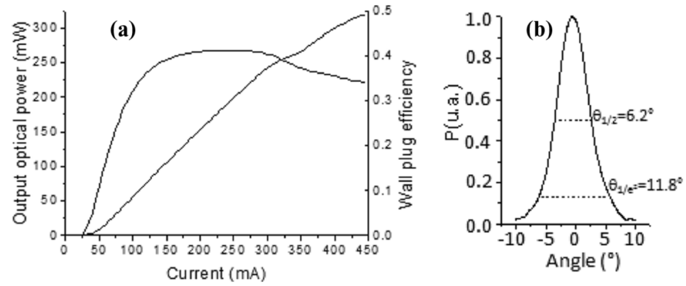


Fig. 2. (a) Light output–current ($L$–$I$) and plug efficiency characteristics for a 2-mm-long AR/HR coated ridge laser diode. (b) Horizontal far field for $I = 280$ mA, $P = 230$ mW.

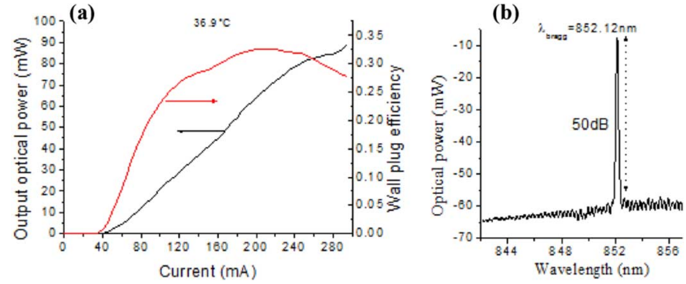


Fig. 3. (a) $L$–$I$ and plug efficiency characteristics of 2-mm-long uncoated DFB laser diode at 36.9 °C. (b) Spectral characteristics of the DFB 2-mm-long laser at 852.12 nm and $T = 36.9$°C.

$(Al_{25\%})$, as shown in Fig. 1. At this particular wavelength and to fully exploit the advantages of the Al-free InGaAsP–GaAs material system, high bandgap confining Al-containing layers are required to bypass any carrier leakage problems. The bandgap difference between the active and cladding layers is significantly higher than what would be commonly possible with a completely Al-free structure. This approach has proven to be effective in lowering carrier leakage to a level similar to that observed in conventional AlGaAs-based lasers.

A GaInP–InGaAsP–GaInP multilayer corresponding to the grating completes the first epitaxial step. The grating structure is defined by holographic photolithography and the pattern is transferred into the first two layers by a methane/hydrogen reactive ion etching process. To obtain a 1 : 3 aspect ratio for the gratings, a typical selective wet etching solution is used followed by thorough cleaning prior to the epitaxial regrowth process. The 1 : 3 aspect ratio is fundamental to achieving maximum coupling coefficiency in second-order DFBs. The epitaxial regrowth step is then carried out to grow the ridge layers (p-AlGaInP and p-GaInP) and a p-GaAs contact layer. In order to obtain a spatial single-mode emission, lateral confinement is provided by 4-$\mu$m-wide ridge diode lasers using typical fabrication process. The cavity length is 2 mm and the front and rear facets are coated with reflection coefficients of around 5% and 95%, respectively (to improve continuous-wave (CW) power). The chips are separated using dicing techniques and are mounted p-down on submounts.

Experiment has been carried out on broad-area lasers initially and also on ridge waveguide devices. Broad-area lasers with a stripe width of 100 $\mu$m were processed. To reduce current injection area, a mesa structure was formed in the stripe region of the contact layer. The wafer is metallized on the n- and p-side junction, and cleaved to form laser bars with different cavity lengths. Individual broad-area chips were bonded in a junction-down configuration (p-down). Diodes with uncoated facets were tested to determine typical parameters such as internal efficiency, internal loss, and transparency current density.

## III. Results and Discussion

### A. Broad-Area Laser Diode

We determine low internal losses ($<3$ cm$^{-1}$), a high internal efficiency (94%) and a low transparency current density (100 A/cm$^2$), which illustrate the very high quality of the InGaAsP active region. We measure a threshold current of 490 mA for a 2-mm-long broad-area coated device, corresponding to the vertical structure without grating layers and grown in one step. We obtain a maximum optical output power of 5.5 W measured at 8.5 A.

A Gaussian shape for the far-field is observed in the perpendicular direction confirming the monomode behavior in this direction. A close conformity is also observed between the simulated and experimental far-field measurement. All these results illustrate the excellent quality of the laser structure.

### B. Fabry–Pérot Ridge Waveguide Laser Diode

Preliminary characterization on the ridge waveguide structure was based on 2-mm-long coated devices with a ridge width of 4 $\mu$m. The power-current characteristic in CW operation of this device is shown in Fig. 2(a). The threshold current is about 46 mA and the slope efficiency is near 0.9 W/A for antireflection (AR)/high-reflectivity (HR) coated facet lasers. Thanks to the compressive-strained active quantum well, the laser operates steadily in the transverse-electric mode (degree of polarization >95%).

We demonstrate the high stability of the beam quality factor [7] in the lateral direction, $M^2$ ($<1.5$) up to 250 mW. The transverse far-field is Gaussian with an FWHM of 32° and full width at $1/e^2$ of 62° which is similar of broad-area laser far field. Both near- and far-field [Fig. 2(b)] profiles in the slow axis measured at injection current of 280 mA (230 mW), are nearly Gaussian shaped with respective full widths at $1/e^2$ of 7 $\mu$m and 11.8° and FWHM of 4 $\mu$m and 6.2°. The lack of beam steering indicates stable fundamental lateral mode operation.

### C. DFB Ridge Waveguide Laser Diode [8]

Following the results obtained on the ridge waveguide structures, DFB ridge lasers were then fabricated with a ridge width of 4 $\mu$m. The power-current characteristic in CW operation at 36.9 °C of this device is illustrated in Fig. 3(a) showing a low threshold of 52 mA, a high slope efficiency of 0.4 W/A, and an

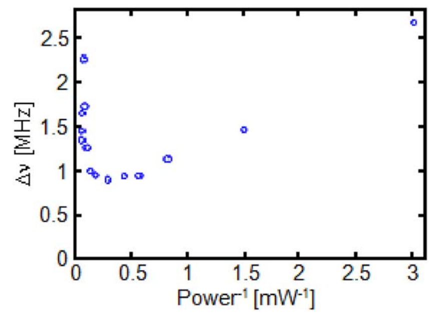


Fig. 4. Variation of measured linewidth with respect to the inverse of optical power.

output optical power of 80 mW at 240 mA for a 2-mm-long uncoated DFB ridge laser. At $D_2$ line wavelength ($P = 40$ mW, $T = 36.9$°C), a $M^2$ value of 1.3 [9] is measured corresponding to a single spatial mode behavior.

Fig. 3(b) shows the cesium transition Bragg wavelength of 852.12 nm. At 37 °C and 852.1 nm, the sidemode suppression ratio (SMSR) is around 50 dB indicating a very good single-mode emission. We demonstrate a very high stability of SMSR with temperature (>30 dB up to 80 °C) and power (>30 dB up to 53 mW at 20 °C).

### *D. Linewidth Measurement*

The spectral linewidths of the DFB lasers were measured using the optical feedback self-mixing interferometric (SMI) technique, as first proposed by Giuliani *et al.* [10]. SMI has recently been developed to carry out measurement of parameters such as the linewidth and the linewidth enhancement factor of semiconductor laser devices [11]. This method is based on the measurement of phase noise in an interferometer. The minimum value of linewidth measurable with a very simple experimental setup is estimated at 0.5 MHz with this method.

Spectral lineshape measurements were taken at various output powers and are shown in Fig. 4. The linewidth close to the threshold current is 2.67 MHz, and it decreases down to 0.9 MHz at 70 mA and 5 mW. An extrapolated power-independent linewidth floor of 0.55 MHz for infinite power is obtained. At high power levels, the linewidth then increases up to 2.25 MHz at 120 mA and 25 mW. This is predicted theoretically [12] and has been observed with similar devices.

Measurement carried out revealed an $\alpha$-factor between 4.8 and 5.3. We obtain generally $\alpha$-factor value around 4. The low spectral linewidth is due to an optimization of the cavity design.

## IV. Conclusion

Low-threshold, high-power, and single-mode operation was demonstrated for 852-nm Al-free active region index guided DFB lasers grown by MOVPE. In particular, we obtain a low threshold current (52 mA) and a slope efficiency of 0.4 W/A at 36.9 °C. We measure an optical power of 80 mW ($I = 240$ mA) in a single spatial mode with the beam quality parameter $M^2$ in the lateral direction of 1.5 at the same temperature. At 240 mA, both near and far field are Gaussian-shaped with respective full widths at $1/e^2$ of 7 $\mu$m and 12.5°. An SMSR greater than 45 dB is measured at 140 mA, 30 mW, 36.9 °C. Further characterization of the laser devices show narrow spectral linewidths measured using the optical feedback SMI technique. A minimum linewidth of 0.9 MHz has been demonstrated. With this particular operating performance, these DFB structures are very good candidates for high-performance laser sources used in applications like atomic clocks (hot Cs atoms) in satellites or on ground. The reduction of linewidth (100–200 kHz) at higher power (100 mW) for DFB laser will be necessary to address directly atom cooling applications.

## Acknowledgment

The authors would like to thank L. Teisseire, Y. Robert, C. Dernazaretian, and A. Lordereau for excellent technical assistance, and C. Vian, D. Holleville, and N. Dimarcq from BNM-SYRTE (Paris Observatory) for fruitful discussions.

## References

[1] H. Wenzel, M. Braun, and J. Fricke, “High-power ridge-waveguide distributed-feedback lasers emitting at 860 nm,” *Electron. Lett.*, vol. 38, no. 25, pp. 1676–1677, Dec. 2002.

[2] A. Kler *et al.*, “852 nm distributed feedback diode lasers for atomic clocks and laser cooling,” in *Proc. CLEO Europe*, Munich, Germany, Jun. 12–17, 2005, Paper CB4-2.

[3] M. Fukuda, M. Okayasu, and J. Temmyo, “Degradation behavior of 0.98-$\mu$m strained quantum well InGaAs/AlGaAs lasers under high-power operation,” *IEEE J. Quantum Electron.*, vol. 30, no. 2, pp. 471–476, Feb. 1994.

[4] S. L. Yellen, A. H. Shepard, C. M. Harding, J. A. Baumann, R. G. Waters, D. Z. Garbuzov, V. Pjataev, V. Kochergin, and P. S. Zory, “Dark-line-resistant, aluminum-free diode laser at 0.8 mu m,” *IEEE Photon. Technol. Lett.*, vol. 4, no. 12, pp. 1328–1330, Dec. 1992.

[5] D. Z. Garbuzov, N. Y. Antonishkis, A. D. Bondarev, A. B. Gulakov, S. N. Zhigulin, N. I. Katsavets, A. V. Kochergin, and E. V. Rafailov, “High-power 0.8 $\mu$m InGaAsP–GaAs SCH SQW lasers,” *IEEE J. Quantum Electron.*, vol. 27, no. 6, pp. 1531–1536, Jun. 1991.

[6] D. Botez *et al.*, “66% CW wallplug efficiency from al-free 0.98 $\mu$m-emitting diode lasers,” *Electron. Lett.*, vol. 32, no. 21, pp. 2012–2013, Oct. 1996.

[7] A. E. Siegman, “New developments in laser resonators,” *Proc. SPIE*, vol. 1224, Optical Resonators, pp. 1–14, 1990, invited paper.

[8] V. Ligeret, S. Bansropun, M. Lecomte, M. Calligaro, O. Parillaud, and M. Krakowski, “Narrow spectral linewidth of Al-free active region DFB laser diodes operating at 852 nm,” in *Proc. CLEO US*, San José, CA, May 6–11, 2007, Paper JWA129.

[9] V. Ligeret *et al.*, “High-power al-free active region ($\lambda = 852$ nm) DFB laser diodes for atomic clocks and interferometry applications,” in *Proc. CLEO US*, Long Beach, CA, May 21–26, 2006, Paper JWB5.

[10] G. Giuliani and M. Norgia, “Laser diode linewidth measurement by means of self-mixing interferometry,” *IEEE Photon. Technol. Lett.*, vol. 12, no. 8, pp. 1028–1030, Aug. 2000.

[11] Y. Yu, G. Giuliani, and S. Donati, “Measurement of the linewidth enhancement factor of semiconductor lasers based on the optical feedback self-mixing effect,” *IEEE Photon. Technol. Lett.*, vol. 16, no. 4, pp. 990–992, Apr. 2004.

[12] H. Olesen *et al.*, “Mode instability and linewidth rebroadening in DFB lasers,” *Electron. Lett.*, vol. 28, no. 5, pp. 444–446, Feb. 1992.